

Short Communication

The Relation between Intergranular Corrosion and Electrochemical Characteristic of Carbon Steel in Carbonic Acid and Sodium Nitrite Solutions

Yong Zhou, Fu an Yan *

Key Laboratory of Green Chemical Process, Ministry of Education, Wuhan Institute of Technology, Wuhan 430073, China

Hubei Key Laboratory of Novel Reactor and Green Chemical Technology, Wuhan Institute of Technology, Wuhan 430073, China

*E-mail: yanfuan1818@163.com

Received: 4 January 2016 / *Accepted:* 8 March 2016 / *Published:* 1 April 2016

The intergranular corrosion (IGC) and electrochemical characteristic of carbon steel in carbonic acid and sodium nitrite solutions was studied with methods of potentiodynamic polarization and metallographic microscope. The relation between intergranular corrosion and electrochemical characteristic was discussed. The occurrence of IGC was observed on the steel surface when the steel was potentiodynamic polarized in carbonic acid and sodium nitrite mixed solution. Carbon steel showed the typical electrochemical characteristic of active-passive-transpassive in the mixed solution, and the initiation and propagation of IGC was observed only when the steel was potentiodynamic polarized in active-passive transition region, passive region and transpassive region. For carbon steel in the mixed solution, the occurrence of IGC was very closely related to the electrochemical characteristic of active-passive transition: carbonic acid induced the dissolution of grain boundaries and sodium nitrite promoted the passivation of crystal grains.

Keywords: carbon steel; intergranular corrosion; electrochemical characteristic; carbonic acid; sodium nitrite

1. INTRODUCTION

Intergranular corrosion (IGC) is one of the most common localized corrosion for metals and alloys [1]. Because of the occurrence of IGC, the bonding force among crystal grains can be weakened seriously [2], and the mechanical strength of metals and alloys can be damaged markedly [3].

At present, studies involving IGC have been mainly focused on stainless steels (SS), nickel alloys and aluminum alloys (AA). For these three materials, the IGC susceptibility is usually showed when they are under the condition of welding process or heated application, so at room temperatures they do not show the IGC susceptibility [4]. One of the important reasons for the presence of IGC susceptibility is sensitization: for SS chromium depletion attributed to the precipitation of Cr_{23}C_6 at grain boundaries [5] and for AA copper depletion due to the precipitation of CuAl_2 at grain boundaries [6]. The passivation ability of grain boundaries is weakened because of the precipitation of some phases, resulting in the formation of micro-galvanic cell between crystal grains and grain boundaries. Jeon et al. [7] studied the effect of Ce addition on the precipitation of bad phases and the associated IGC resistance of 27Cr-7Ni hyper duplex SS. The authors reported that on the one hand the addition of Ce element to the base SS significantly decreased the amount of bad phase precipitated, which was the sigma phase composed of Cr_{23}C_6 ; on the other hand, the addition of Ce element to the base SS also inhibited the decrease of the IGC resistance. Tachibana et al. [8] studied the effects of hot rolling and following cooling condition on the IGC behavior for 625 nickel base alloy. The authors reported the IGC resistance of the Ni-alloy at finishing rolling temperature from 800 to 900 °C was almost similar to that at solution treatment temperature. At finishing rolling temperature of 750 °C, the corrosion rate of the Ni-alloy increased due to sensitization by precipitation. However, at finishing rolling temperature of 1000 °C, the corrosion rate of the Ni-alloy also increased, which was not due to sensitization. The possible mechanism was preferential corrosion occurred at recrystallized grain boundaries attributed to an anodic reaction concentration. Dick et al. [9] studied the corrosion of the friction stir lap joint for AA7050-T76511 on AA2024-T3 using the scanning vibrating electrode technique. The authors reported that AA2024 heat-affected zone was the most IGC susceptibility region, and IGC was less intense than on parent AA2024-T3 alloy.

However, carbon steels are a kind of metals and alloys which do not show obvious IGC susceptibility, and few reports involve the IGC of carbon steels [10,11]. Kupper et al. [10] studied the IGC of carbon steels with 0.003-2.5 wt% phosphorus in nitrate solutions at high temperature and reported that the IGC susceptibility increased with the increase of phosphorus content, which was very closely related to the phosphorous concentration at grain boundaries. The main reason of IGC was that the phosphorus segregation at the grain boundaries prevented the formation of protective passive film on the steel surface. Krauschick et al. [11] studied the IGSCC of carbon steels with 0.003-2.0 wt% phosphorus in nitrate and sulfate solutions and reported that phosphorus prevented the formation of protective oxide film on the steel surface, which was also attributed to the segregation of phosphorus at the grain boundaries.

In our previous study [12], the occurrence of IGC was observed on a carbon steel surface when the steel was potentiodynamic polarized in carbonic acid and sodium nitrite mixed solution. In this paper, the intergranular corrosion and electrochemical characteristic of carbon steel in the mixed solution is studied with methods of potentiodynamic polarization and metallographic microscope. The relation between intergranular corrosion and electrochemical characteristic is discussed also.

2. EXPERIMENTAL

2.1 Material and solution

The studied material was carbon steel with the following chemical composition (wt %): C, 0.16; Mn, 0.53; Si, 0.30; S, 0.045; P, 0.015, and Fe. Samples were manually abraded up to 1000 grit with SiC abrasive papers, rinsed with de-ionized water and degreased in acetone. The samples were coated with epoxy resin, leaving 0.25 cm^2 exposed to solution as the working electrode.

There were three test solutions applied. Solution I was a carbonic acid solution: CO_2 gas was purged into 200 ml de-ionized water until the CO_2 saturated condition was reached. Solution II was a sodium nitrite solution: 0.14 g sodium nitrite was added into 200 ml de-ionized water and a 0.01 mol/L sodium nitrite solution was obtained. Solution III was a carbonic acid and sodium nitrite mixed solution: 0.14 g sodium nitrite was added into Solution I to obtain a mixed solution.

2.2 Electrochemical measurement

The electrochemical measurement of polarization was carried out using a CS350 electrochemical workstation. Before each polarization test, the working electrode was immersed in solution for a certain time to ensure the open circuit potential (OCP) to be stable. According to our previous study [12], the potential scanning rate of 0.1 mV/s was applied to ensure the occurrence of IGC. A typical three electrode system was used for the polarization tests. The system was composed of a saturated calomel electrode (SCE) as reference electrode, a platinum sheet as counter electrode and the carbon steel sample as working electrode. All of the polarization tests were carried out at ambient temperature. Further, after the first polarization curve test was finished, the same working electrode without any treatment was polarized in Solution III to obtain the second polarization curve.

2.3 Metallographic microscope observation

The surface morphologies of the carbon steel samples were observed with a 4XC metallographic microscope instrument.

3. RESULTS AND DISCUSSION

3.1 Electrochemical characteristic and surface metallographic morphology

Fig. 1 shows the polarization curves of carbon steel in carbonic acid solution, sodium nitrite solution and the mixed solution. In carbonic acid solution, carbon steel showed the electrochemical characteristic of active dissolution and the anodic current density increased gradually with the positive shift of potential. From the polarization curve, it can be obtained that for carbon steel in carbonic acid solution the corrosion potential is about $-0.68 \text{ V}_{\text{SCE}}$ and the corrosion current density is about 2.17

mA/cm². Due to the enrichment of carbon dioxide, carbonic acid was a relative strong corrosion medium, resulting in a higher corrosion frequency and a larger corrosion rate for metals and alloys. Burstein et al. [13] studied the corrosion of pipeline steel in carbon dioxide solution and reported that the steel showed the similar electrochemical characteristic and the approximate values of corrosion potential and corrosion current density.

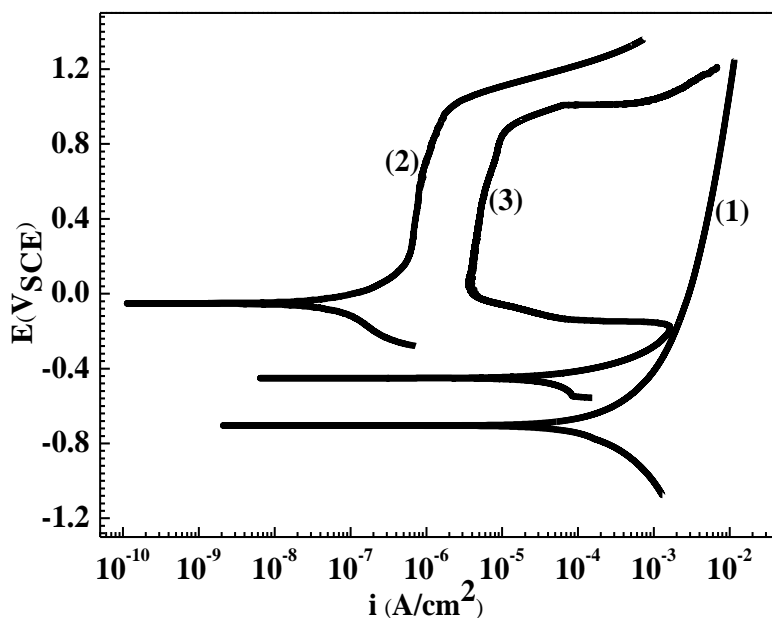


Figure 1. Polarization curves of carbon steel in carbonic acid solution (1), sodium nitrite solution (2) and the mixed solution (3).

Fig. 2 shows the surface metallographic morphology of the sample polarized to 1.2 V_{SCE} in carbonic acid solution. There is no sign of IGC observed on the sample surface, but some scratches derived from mechanical action of abrasive paper can be seen only, indicating that IGC did not occur when carbon steel showed the active characteristic in the studied solution.

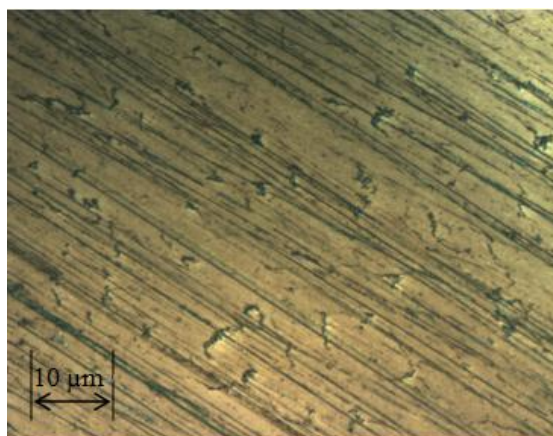


Figure 2. Surface metallographic morphology of carbon steel polarized to 1.2 V_{SCE} in carbonic acid solution.

From Fig. 1, in sodium nitrite solution, carbon steel showed the electrochemical characteristic of spontaneous passivation and obvious passive region could be observed on the polarization curve. From the polarization curve, it can be obtained that for carbon steel in sodium nitrite solution the corrosion potential is about $-0.05 V_{SCE}$ and the corrosion current density is about $0.54 \mu A/cm^2$. For the steel, the corrosion potential and the corrosion current density in sodium nitrite solution are respectively more positive and lower than those in carbonic acid solution, which was attributed to the inhibitive property of nitrite. According to previous studies [14-16], nitrite was a good corrosion inhibitor for steels in neutral and alkaline corrosion medium. The inhibitive mechanism of nitrite was attributed to its strong oxidability, and a stable oxide film could be formed and remained on steels surface under the combined action between nitrite and iron.

Fig. 3 shows the surface metallographic morphology of the sample polarized to $1.2 V_{SCE}$ in sodium nitrite solution. It can be observed that the surface metallographic morphology of the sample polarized in sodium nitrite solution is similar to that polarized in carbonic acid solution: only the presence of scratches can be observed and there is no sign of IGC. Therefore, it is seen that IGC did not occur when carbon steel showed the passive characteristic in the studied solution.

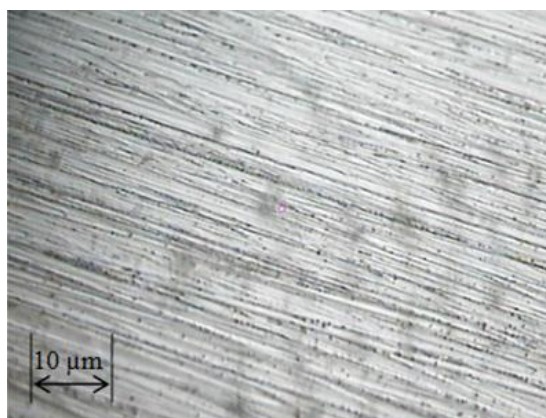


Figure 3. Surface metallographic morphology of carbon steel polarized to $1.2 V_{SCE}$ in sodium nitrite solution.

However, in carbonic acid and sodium nitrite mixed solution, carbon steel showed the typical electrochemical characteristic of active-passive-transpassive, and the anodic polarization curve can be divided into four parts: active region, active-passive transition region, passive region and transpassive region, as showed in Fig. 1. In the active region, the current density increased gradually with the positive of potential, and carbon steel showed the electrochemical characteristic of active dissolution similar to the characteristic in carbonic acid solution. In the active-passive transition region, the current density started to decrease after it reached the critical passive current density ($1.5 mA/cm^2$) corresponding to the active-passive transition potential, then the current density decreased sequentially until the passive current density ($4.0-5.0 \mu A/cm^2$) corresponding to the initial passive potential. In the passive region, the current density remained stable at the passive current density regardless of the positive shift of potential. In the transpassive region, the current density increased once again with the positive shift of potential when the transpassive potential was reached. According to our previous study on the anodic passivation behavior of carbon steel in carbon dioxide saturated solution containing

nitrite anions [17], the active-passive characteristic was attributed to the combined action between carbon dioxide and sodium nitrite, and the passivation of carbon steel was due to the formation of a protective Fe_2O_3 passive film under corrosion products layer.

Fig. 4 shows the surface metallographic morphology of the sample polarized to $1.2 \text{ V}_{\text{SCE}}$ in the mixed solution. From the surface metallographic morphology showed in Fig. 4, the occurrence of IGC can be observed, indicating that IGC could occur when carbon steel showed the active-passive-transpassive characteristic in the studied solution.

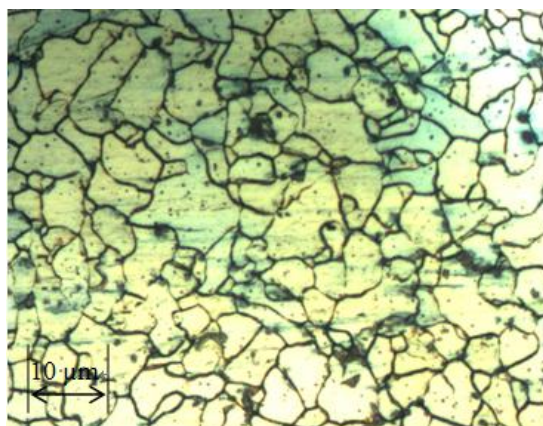


Figure 4. Surface metallographic morphology of carbon steel polarized to $1.2 \text{ V}_{\text{SCE}}$ in carbonic acid and sodium nitrite mixed solution.

3.2 Relation between IGC and potential in the mixed solution

From the above results, it is seen that IGC occurred on the steel surface when the steel was potentiodynamic polarized in carbonic acid and sodium nitrite mixed solution. However, the polarization curve of carbon steel in the mixed solution was relatively complicated, which was composed of four parts showed in Fig. 1. In order to understand the detailed information of IGC, some carbon steel samples were potentiodynamic polarized to different potentials in the mixed solution, and the samples surface was observed by metallographic microscope.

Fig. 5 shows the surface metallographic morphologies of carbon steel samples polarized to different potentials in the mixed solution. Fig. 5a shows the surface metallographic morphology of the sample polarized to the active-passive transition potential ($-0.20 \text{ V}_{\text{SCE}}$) in the mixed solution, which is similar to the surface metallographic morphology of the sample polarized in carbonic acid solution showed in Fig. 2. In Fig. 5a and Fig. 2, no sign of IGC on the samples surface can be observed. Fig. 5b showed the surface metallographic morphology of the sample polarized to the initial passive potential ($0.04 \text{ V}_{\text{SCE}}$). From Fig. 5b, the occurrence of IGC can be observed obviously on the sample surface. Similar surface metallographic morphology is also observed in Fig. 5c, which is the surface metallographic morphology of the sample polarized to the transpassive potential ($0.10 \text{ V}_{\text{SCE}}$). The results showed in Fig. 5b and 5c indicate that for carbon steel in the mixed solution IGC has been occurred on the steel surface before the steel was polarized in the passive region and the transpassive region. At the same time, it is seen from Fig. 5a that IGC do not occur in the steel surface when the

steel was polarized in the active region. Therefore, it can be inferred that the initiation of IGC possibly occurred when the steel was polarized in the active-passive transition region. In order to confirm this assumption, a sample was polarized to a middle potential value about $-0.08 V_{SCE}$ between the active-passive transition potential and the initial passive potential, and the sample surface was observed with metallographic microscope showed in Fig. 5d. In Fig. 5d, it is seen that IGC has been occurred on the sample surface, but the corrosion damage of grain boundaries at the middle potential is lower than that at the initial passive potential or at the transpassive potential, indicating that the initiation and propagation of IGC for carbon steel in the mixed solution was very closed related to the potential. Similar results that potential played a critical role in IGC studies were usually involved in double loop electrochemical potentiodynamic reactivation (DL-EPR) test, which was applied to evaluate IGC susceptibility for stainless steels and nickel alloys [21]. However, it must be paid attention to that in this work the IGC occurred on the steel surface when the potential scanning was through in the active-passive transition region, but during the process of DL-EPR test the occurrence of IGC was observed on stainless steels or nickel alloys surface when the potential scanning was reversed from the passive region to the reactivation region.

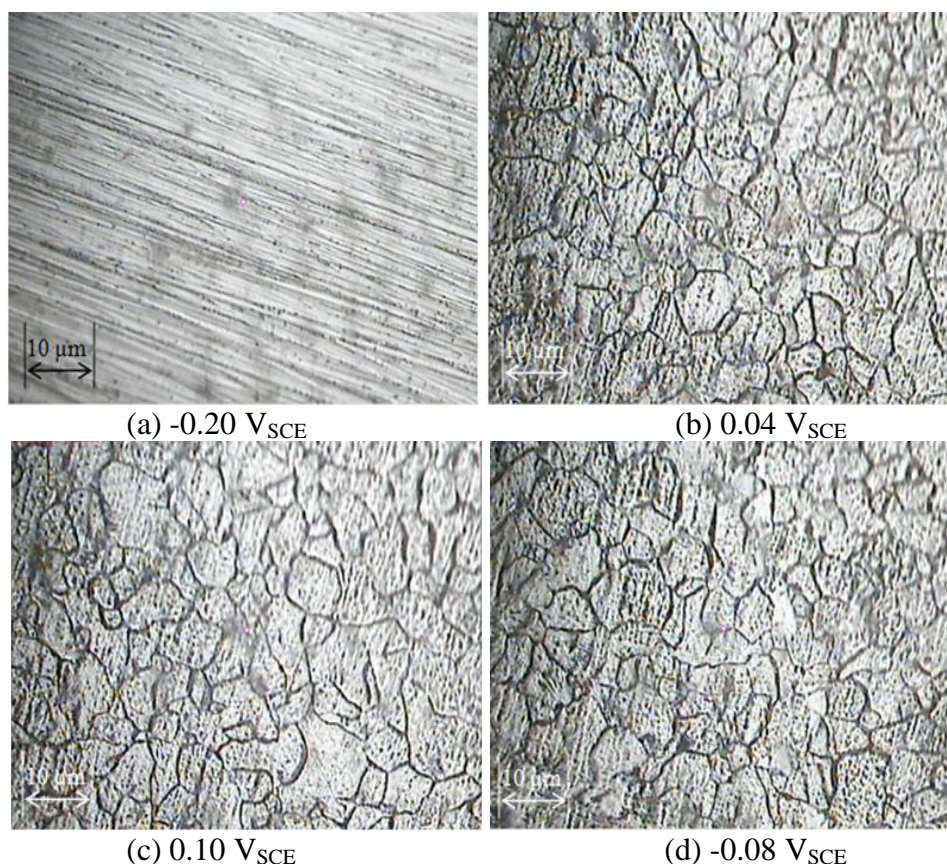
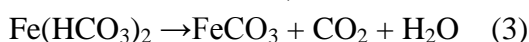
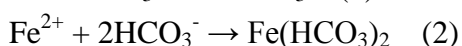
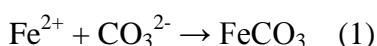


Figure 5. Surface metallographic morphologies of carbon steel polarized to different potentials in carbonic acid and sodium nitrite mixed solution: (a) $-0.20 V_{SCE}$, (b) $0.04 V_{SCE}$, (c) $0.10 V_{SCE}$ and (d) $-0.08 V_{SCE}$.

3.3 Comparison of electrochemical characteristic

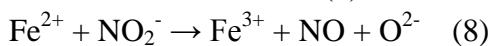
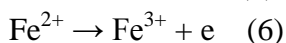
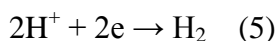
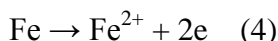
In order to analyze the electrochemical characteristics of carbon steel in carbonic acid, sodium nitrite and the mixed solution, the three polarization curves are contrasted. From Fig. 1, it is obviously seen that the polarization curve in the mixed solution is located between the curve in carbonic acid solution and the curve in sodium nitrite solution. At the same time, the value of corrosion potential and the value of corrosion current density in the mixed solution are between the corresponding values in carbonic acid solution and in sodium nitrite solution, which was attributed to the aggressive property of carbonic acid [18] and the inhibitive property of sodium nitrite [19].

On the one hand, carbon steel showed the electrochemical characteristic of active dissolution at the whole region of the curve measured in carbonic solution and at the active region of the curve measured in the mixed solution. According to previous study [13], there are three reactions occurring as follows:



Therefore, it can be inferred that the active characteristic of carbon steel at the active region in the mixed solution was attributed to the effect of carbonic acid.

On the other hand, the electrochemical characteristic of carbon steel at the passive region of the curve measured in the mixed solution is similar to that at the whole region of the curve measured in sodium nitrite solution, so it is also inferred that the anodic passive characteristic of carbon steel at the passive region in the mixed solution was due to the effect of sodium nitrite. According to our previous study [17], there are four reactions occurring as follows:



3.4 Relation between intergranular corrosion and electrochemical characteristic

From the above results, it is seen that the occurrence of IGC was observed on the steel surface when the steel showed the active-passive-transpassive characteristic and was polarized in the active-passive transition region in the mixed solution. The relation between intergranular corrosion and electrochemical characteristic may be as follows.

In carbonic acid and sodium nitrite mixed solution, with the positive shift of potential, the anodic polarization curve of carbon steel was composed of four obvious parts: active region, active-passive transition region, passive region and transpassive region. In the active region, the current density increased gradually with the positive shift of potential due to the effect of carbonic acid. The air-formed oxide film on the steel surface was dissolved, resulting in that crystal grains and grain boundaries exposed to the mixed solution directly. When the potential positively moved to the active-

passive transition potential, the current density reached the critical passive current density simultaneously, and the polarization curve entered the active-passive transition region. However, the different composition between crystal grains and grain boundaries was quite obvious: crystal grains were composed of Fe, C and O mainly but grain boundaries were composed of Fe, C, O, Mn and Si. The presence of Mn and Si at grain boundaries was adverse to the occurrence of passivation, which was attributed to the grain boundary segregation [20]. Therefore, when the steel was polarized in the active-passive transition region, crystal grains showed the passive status due to the combined action of iron and nitrite, but grain boundaries still showed the active status attributed to the enrichment of Mn and Si, resulting in the electrochemical inhomogeneity and the formation of micro-galvanic cell between crystal grains and grain boundaries. In the active-passive transition region, the current density decreased gradually with the positive shift of potential along with the propagation of IGC and the consumption of Mn and Si. After that, when the potential positively moved to the initial passive transition potential, the current density reached the passive current density simultaneously, and the polarization curve entered the passive region. Besides crystal grains, grain boundaries also got passivation, which might be attributed to the complete consumption of Mn and Si at grain boundaries. Therefore, in the passive region, the current density remained stable at the passive current density regardless of the positive shift of potential. Finally, the current density increased sharply once again with the positive of potential when the potential moved to the transpassive potential, which might be due to new electrode reactions occurred on the steel surface.

In order to confirm the effect of Mn and Si at grain boundaries on IGC, a steel sample was potentiodynamic polarized twice in the mixed solution. In the first polarization test, carbon steel showed the typical electrochemical characteristic of active-passive-transpassive showed in Fig. 1, while in the second polarization curve carbon steel showed the electrochemical characteristic of spontaneous passivation without the anodic current peak, as showed in Fig. 6. The above results of polarization indicate that the elements of Mn and Si at grain boundaries have been consumed completely during the process of first polarization test, so the passivation of crystal grains and grain boundaries occurred simultaneously during the second polarization test.

Therefore, it is seen that for carbon steel in carbonic acid and sodium nitrite mixed solution the occurrence of IGC is very closely related to the electrochemical characteristic of active-passive-transpassive. Similar active-passive transition characteristic was also reported on DL-EPR test for stainless steels and nickel alloys. During the process of DL-EPR test, the occurrence of IGC was observed when the potential scanning was reversed to the reactivation region, which was attributed to the precipitation of some phases on grain boundaries when stainless steels and nickel alloys were under the condition of welding process or heated application. For carbon steel and stainless steel, the mechanism of IGC was totally different although the similar electrochemical characteristic of active-passive transition was showed. For carbon steel in this work, the presence of aggressive and inhibitive species in environmental medium played a significant role in the occurrence of IGC; however, for stainless steels, the occurrence of IGC was mainly attributed to the change of chemical composition and organization structure during the process of welding process or heated application.

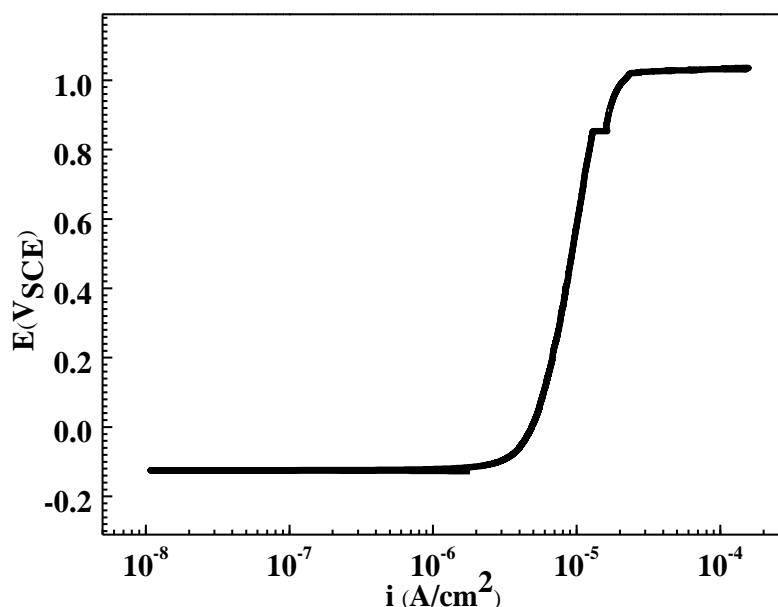


Figure 6. Second polarization curve of carbon steel in carbonic acid and sodium nitrite mixed solution after the first polarization test was finished.

4. CONCLUSIONS

(1) For carbon steel in carbonic acid and sodium nitrite solution, the steel showed the electrochemical characteristic of active-passive-transpassive and the intergranular corrosion was observed on the steel surface when the steel was potentiodynamic polarized in active-passive transition region, passive region and transpassive region.

(2) The occurrence of intergranular corrosion was very closed related to the active-passive characteristic in carbonic acid and sodium nitrite solution, and carbonic acid induced the dissolution of grain boundaries and sodium nitrite promoted the passivation of crystal grains.

(3) The initiation and propagation of intergranular corrosion mainly occurred when the steel was polarized in the active-passive transition region. The corrosion damage of grain boundaries showed a little change when the steel was polarized in the passive region.

References

1. D.L. Engelberg, *Shreir's Corrosion*, 2 (2010) 810.
2. D.A. Little, B.J. Connolly and J.R. Scully, *Corrosion Science*, 49 (2007) 347.
3. M.A. Arafin and J.A. Szpunar, *Corrosion Science*, 51 (2009) 119.
4. C. Garcia, M.P.de Tiedra, Y. Blanco, O. Martin and F. Martin, *Corrosion Science*, 50 (2008) 2390.
5. J.M. Aquino, C.A. Della Rovere and S.E. Kuri, *Corrosion Science*, 51 (2009) 2316.
6. S. Jain, M.L.C. Lim, J.L. Hudson and J.R. Scully, *Corrosion Science*, 59 (2012) 136.
7. S. Jeon, D.H. Hur, H.J. Kim and Y.S Park, *Corrosion Science*, 90 (2015) 313.

8. S. Tachibana, Y. Kuronuma, T. Yokota, K. Yamada, Y. Moriya and C. Kami, *Corrosion Science*, 99 (2015) 125.
9. J.C.B. Bertonecello, S.M. Manhabosco and L.F.P. Dick, *Corrosion Science*, 94 (2015) 359.
10. J. Kupper, H. Erhart and H.J. Grabke, *Corrosion Science*, 21 (1981)227.
11. H.J. Krautschick, H.J. Grabke and W. Diekmann, *Corrosion Science*, 28 (1988) 251.
12. Y. Zhou and Y. Zuo, *Electrochimica Acta*, 154 (2015) 157-165.
13. B.R. Linter and G.T. Burstein, *Corrosion Science*, 41 (1999) 117.
14. M. Reffass, R. Sabot, M. Jeannin, C. Rerziou and P. Refait, *Electrochimica Acta*, 52 (2007) 7599.
15. D.Y. Lee, W.C. Kim and J.G. Kim, *Corrosion Science*, 64 (2012) 105.
16. Z.H. Dong, W. Shi, G.A. Zhang and X.P. Guo, *Electrochimica Acta*, 56 (2011) 5890.
17. Y. Zhou and Y. Zuo, *Journal of the Electrochemical Society*, 162 (2015) 47.
18. S.D. Zhu, A.Q. Fu, J. Miao, Z.F. Yin, G.S. Zhou and J.F. Wei, *Corrosion Science*, 53 (2011) 3156.
19. Z.H. Dong, W. Shi and X.P. Guo, *Corrosion Science*, 53 (2011) 1322.
20. Y.P. Xie and S.J. Zhao, *Journal of Nuclear Materials*, 445 (2014) 43.
21. G.H. Aydogdu and M.K. Aydinol, *Corrosion Science*, 48 (2006) 3565.

© 2016 The Authors. Published by ESG (www.electrochemsci.org). This article is an open access article distributed under the terms and conditions of the Creative Commons Attribution license (<http://creativecommons.org/licenses/by/4.0/>).